Isotope Geochronology in the High-grade Metamorphic Precambrian of Southwestern Norway: New Data and Reinterpretations

J. B. W. WIELENS, P. A. M. ANDRIESSEN, N. A. I. M. BOELRIJK, E. H. HEBEDA, H. N. A. PRIEM, E. A. TH. VERDURMEN & R. H. VERSCHURE

Wielens, J. B. W., Andriessen, P. A. M., Boelrijk, N. A. I. M., Hebeda, E. H., Priem, H. N A., Verdurmen, E. A. Th. & Verschure, R. H. 1980: Isotope Geochronology in the high-grade metamorphic Precambrian of southwestern Norway: new data and reinterpretations. *Norges geol. Unders. 359,* 1–30.

A new series of isotopic age data is reported from the high-grade metamorphic Precambrian in S. W. Norway, mainly from the Sirdal–Ørsdal area. U-Pb investigations on suites of zircons from three augen gneisses and a pyroxene syenite produce discordias with upper intercepts between 1070 and 1030 Ma; these ages are assigned to the highest-grade phase of Sveconorwegian metamorphism, M2, induced by the intrusion of the older part of the Bjerkreim–Sokndal lopolith. Some zircon fractions from another pyroxene syenite and a garnetiferous migmatite contain an inheritance of old radiogenic lead, but no conclusions are possible regarding the age of the older component. The lower intercepts of the discordia trajectories are interpreted as reflecting episodic loss of radiogenic lead in the Palaeozoic, probably in relation to the nearby belt of Caledonian orogenesis and/or post-orogenic uplift; the lead-loss event is tentatively correlated with the M4 phase of incipient very-low-grade metamorphism.

Whole-rock Rb–Sr investigations on eleven garnetiferous migmatites, ten granulitic gneisses and six granitic migmatites do not produce isochron relationships. The data-points of the garnetiferous migmatites scatter within an envelope with boundaries of about 1500 and 1100 Ma, suggesting a substantial pre-Sveconorwegian history. The granulitic gneisses and granitic migmatites display rough linear arrangements suggesting a fairly large degree of Sr isotopic equilibration through each suite of samples about 1215 and 930 Ma ago, respectively; it is conceivable that they reflect the M1 and M3 phases of Sveconorwegian metamorphism.

Earlier published Rb–Sr data of the younger part of the Bjerkreim–Sokndal lopolith are reinterpreted. The isotopic ages (whole-rocks Rb–Sr, zircons U–Pb, hornblendes K–Ar) are compatible with an intrusion of this phase about 950 Ma ago.

K–Ar analyses are reported from seventeen hornblendes and ten biotites. Sixteen hornblendes yield ages between about 970 and 940 Ma, and nine biotites between about 880 and 850 Ma. The ages are interpreted as cooling ages after the culmination of the last phase of Sveconorwegian metamorphism (M3).

A revised tentative geochronological column is proposed for some major events in the geological history of S. W. Norway.

J. B. W. Wielens, P. A. M. Andriessen, N. A. I. M. Boelrijk, E. H. Hebeda, H. N. A. Priem, E A. Th. Verdurmen & R. H. Verschure, Z. W. O. Laboratorium voor Isotopen-Geologie, De Boelelaan 1085, 1081 HV Amsterdam, The Netherlands

1. Introduction

The Precambrian basement of southwestern Norway forms part of the Sveconorwegian zone of the Baltic Shield. This zone is geochronologically charac-

terized by ages in the range from about 1200 to 850 Ma (e.g. Neumann 1960, Kratz et al. 1968). It occupies the whole southwestern part of the Shield and extends presumably northward on the continental shelf along the Norwegian coast (Reymer et al. 1980).

Since 1963 the Precambrian basement of southwestern Norway has been the subject of investigation by research teams of Utrecht State University (Tobi 1965, Hermans et al. 1975). As an offspring of this work an isotopic dating investigation was initiated by the Z. W. O. Laboratorium voor Isotopen-Geologie, Amsterdam. The first results of the dating work, including Rb–Sr data, K–Ar dates and the U–Pb analysis of one suite of zircons, have been reported by Versteeve (1975). In the present paper the results are reported of continued isotope geochronological research, mainly in the Sirdal–Ørsdal area (Fig. 1).

2. Geological setting

The Sirdal—Ørsdal area has been the site of several phases of high-grade metamorphism (including migmatization), intense deformation and igneous activity. In its simplest form the basement can be divided into two groups of rocks, a plutonic complex and a high-grade metamorphic association (Hermans et al. 1975).

The plutonic complex may be subdivided into:

A. A number of anorthositic bodies of different ages (Michot 1961, Michot & Michot 1969, Duchesne & Demaiffe 1978).

B. The Bjerkreim–Sokndal lopolith, a layered intrusion. Two phases are distinguished, the younger phase unconformably lying upon the older (Rietmeijer 1979). The older phase consists of folded anorthosite and (leuco)norite, and can be subdivided into five major rhythms. The younger phase has a monzonitic composition and is subdivided into a lower quartz-poor and an upper quartz-rich phase, locally separated by a zone containing xenoliths. On the basis of pyroxene thermometry the intrusion temperature may be estimated at about 1000 °C for the youngest phase (crystallization temperature of the Ca-poor pyroxenes between 1050 ± 100 °C and 950 ± 100 °C, Rietmeyer 1979) and somewhat higher for the oldest phase.

The high-grade metamorphic terrain surrounds the plutonic complex. It consists of intricately folded and migmatized rocks with intercalated igneous intrusives. Five mappable units are distinguished in the area covered by Fig. 1:

C. The charnockitic and granitic migmatites, ranging in aspect from predominantly massive to banded. In the banded parts the melanocratic bands consist mainly of amphibolites and (leuco)norites.

D. The garnetiferous migmatites, characterized by an abundance of garnets and other alumina-rich minerals suggesting a pelitic origin. Rocks of this unit

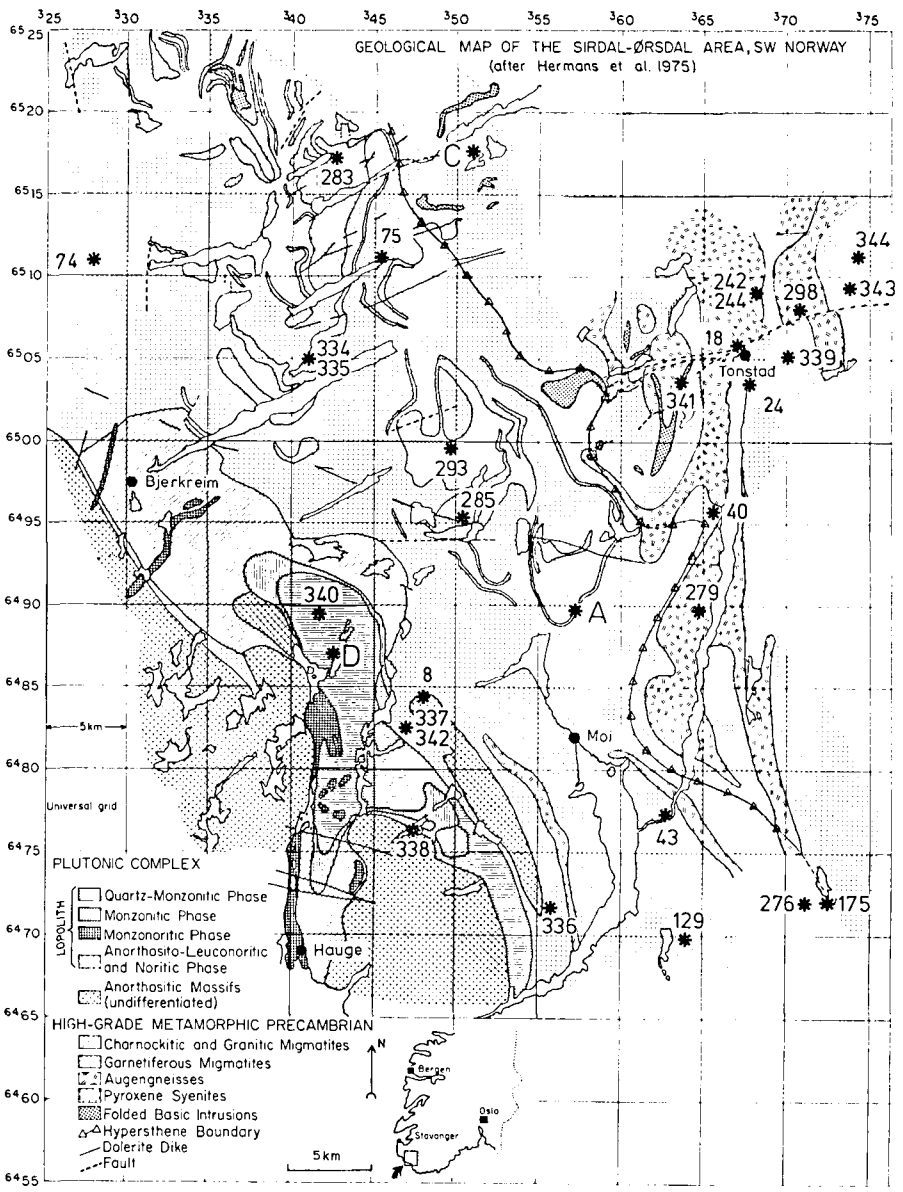

Fig. 1. Geological map of the Sirdal–Ørsdal area (after Hermans et al. 1975), showing the locations of the samples investigated in this study. A, eleven samples from the garnetiferous migmatites, C, ten samples from the granulitic gneisses, D, seven samples from the (quartz-) monzonitic phase of the Bjerkreim–Sokndal lopolith. Location B, six samples from the granitic gneisses near Sinnes, lies north of the map area (NGO grid coordinates 3732–65314).

occupy extensive areas or occur as narrow, folded bands between the charnockitic migmatites. No sedimentary structures have been recognized.

E. The augen gneisses, mainly occurring in the terrain of the granitic migmatites. They occupy large areas and range in aspect from fairly massive

to gneissic. Occasionally, the augen gneisses show a gradual transition into the migmatites.

G. The Gloppurdi and Botnavatn igneous complexes, composed mainly of (olivine-)clinopyroxene syenites and clinopyroxene granites.

H. The folded basic intrusions, forming relatively small masses of biotite noritic composition.

At least four phases of metamorphism have been recognized (Maijer et al. in prep.). First there was a phase of regional metamorphism under conditions of upper amphibolite facies, M1 (biotite, garnet, sillimanite, perthitic K-feldspar), associated with migmatization. This phase probably affected the Precambrian basement all over S. W. Norway. Then the high temperature of the lopolithic magma induced high-temperature/intermediate-pressure granulite facies conditions in the adjacent rocks over the greater part of the investigated area, M2 (orthopyroxene, osumilite, cordierite, green spinel, magnetite, mesoperthitic K-feldspar), locally associated with migmatization. This metamorphism resulted in a gradation of the main metamorphic imprint to the north-east from granulite facies (charnockitic migmatites) to amphibolite facies (granitic migmatites); orthopyroxene is rarely found in the leucocratic rocks east of the so-called 'hypersthene boundary' (Dahlberg 1969). Next there was a phase of metamorphism under conditions of lower granulite to upper amphibolite facies, M3 (biotite, orthopyroxene, garnet, sillimanite, orthoclase, plagioclase). Finally, the rocks were affected by a retrograde phase of incipient very-low-grade metamorphism, M4, as evidenced by the local occurrence of minerals characterizing the pumpellyite-prehnite facies (pumpellyite, prehnite, stilpnomelane).

An age of about 1200 Ma has been assigned to the M1 phase on the basis of several isotopic datings at different places in southern Norway (Versteeve 1975). The other phases are thought to have taken place about 1000–900 Ma ago (Versteeve 1975).

Four phases of folding have been distinguished, D1–D4, varying from intricate isoclinal folding to gentle flexural folding (Hermans et al. 1975). The third phase, D3, is the most conspicuous and is characterized by N–S or NW–SE trending axes and axial planes dipping to the east.

The area is intersected by younger faults and two sets of dolerite dikes, one trending WNW–ESE and the other ENE–WSW.

3. Previous geochronological work

Isotope geochronological investigations in the high-grade metamorphic Precambrian of S. W. Norway have been reported by Michot & Pasteels (1968), Pasteels & Michot (1975), Versteeve (1975), Pedersen et al. (1978), and Pasteels et al. (1979). Most ages characteristically fall in the Sveco-norwegian range of 1200 to 850 Ma, but a few analyses suggest a substantially

higher age record. From the charnockitic migmatites two pre-Sveconorwegian whole-rock Rb–Sr ages have been reported, one of about 1450 Ma in Drangsdalen (Versteeve 1975) and the other of about 1420 Ma north of the plutonic complex (Pasteels & Michot 1975). In both cases the constituent zircons display Sveconorwegian ages (1250 and 1160 Ma, respectively). Other indications for a pre-Sveconorwegian history have been found in the Lyngdal granitic gneiss east of Farsund, where the zircons yield U–Pb ages of 1475 to 1560 Ma (Pasteels & Michot 1975), and in gneisses and granites east of Sauda, where Rb–Sr whole-rock isochrons have been reported of 1520 ± 30 Ma (Berg 1977) and 1477 ± 35 Ma (D. van der Wel, in Sigmond 1978).

The Sveconorwegian geochronology of the Sirdal–Ørsdal area, as far as presently known, may be summarized as follows:

1. The U–Pb discordia age of $1250 \pm {}^{115}_{70}$ Ma obtained on a suite of zircons from a charnockitic sample in Drangsdalen has been related to the older phase of upper amphibolite facies metamorphism (Versteeve 1975), but the data are interpreted differently in this study (chapter 6.5.).
2. A whole-rock Rb–Sr analysis of a suite of samples from the Gloppurdi igneous complex yields an age of 1180 ± 70 Ma with a rather high initial $^{87}Sr/^{86}Sr$ ratio of 0.7103 ± 0.0032 (Versteeve 1975).
3. Most whole-rock Rb–Sr systems of the charnockitic migmatites reveal a severe disturbance during the high-grade metamorphism. At two localities suites of samples collected within a small area indicate ages of 930 ± 25 Ma and 980 ± 85 Ma, both with high initial $^{87}Sr/^{86}Sr$ ratios of about 0.72; they are interpreted as reflecting Sr isotopic equilibration (Versteeve 1975).
4. The whole-rock Rb–Sr data of the (quartz-)monzonitic phase of the Bjerkreim–Sokndal lopolith have been regarded by Versteeve (1975) as indicating an age of 842 ± 30 Ma, but the data are interpreted differently in this study (chapter 8). Another set of Rb–Sr data, obtained by Pasteels et al. (1979), shows a nearly identical age of 857 ± 21 Ma. U–Pb measurements on zircons from these rocks, however, indicate an age of about 950 Ma (Pasteels & Michot 1975, Pasteels et al. 1979).
5. K–Ar and Rb–Sr analyses of osumilite from a garnetiferous migmatite near Vikeså yield ages of about 985 Ma and 950 Ma, respectively; they are interpreted as cooling ages (Maijer et al. in prep.).
6. A hornblende K–Ar age of 1170 Ma has been related to the older phase of upper amphibolite facies metamorphism (Versteeve 1975), but this age is interpreted differently in this study (chapter 9.1). Two other hornblende ages of about 940 Ma have been interpreted as cooling ages (Versteeve 1975).
7. Biotites display Rb–Sr and K–Ar ages between about 900 and 840 Ma; they have been interpreted as cooling ages (Versteeve 1975). In a narrow zone along the front of the Caledonian nappe system, north of the map area of Fig. 1, secondary green biotites with Rb–Sr and K–Ar ages of about 400 Ma occur side by side with the Sveconorwegian brown biotites (Verschure et al. 1979, 1980).

4. Present geochronological investigations

From the earlier investigations it is evident that the Rb–Sr systems in the Sirdal–Ørsdal area have retained very little of the pre-Sveconorwegian age record. The main purpose of this study was to examine whether U–Pb zircon systems could provide means of looking through the Sveconorwegian metamorphic veil. Six suites of zircons from different rock types were therefore investigated, along with two apatites. Moreover, to supplement the work by Versteeve (1975), whole-rock Rb–Sr analyses were made of three suites of rocks from the high-grade metamorphic basement, as well as K–Ar determinations on 17 hornblendes and 10 biotites. The mineral ages should provide further insight into the timing of the cooling history following the climax of the last phase of Sveconorwegian high-grade metamorphism.

5. Experimental procedures and constants

5.1. U-Pb ANALYSIS

Rock samples of about 20 kg were crushed, ground and sieved to a particle size below 250 μm. The zircons were recovered by, successively, density separation using bromoform with a large overflow centrifuge (a modified version of the type described by Verschure & IJlst 1966a), magnetic separation with a modified Frantz isodynamic separator (Verschure & IJlst 1969) after removal of the magnetic ore grains, density separation using diiodomethane with a laboratory overflow centrifuge (IJlst 1973a, 1973b), and density separation with Clerici solution using a funnel. Pyrite, if present, was removed from the concentrate by a modified type of the dielectric separator described by Verschure & IJlst (1966b). The zircon concentrates were sieved into size fractions using specially designed sieves with oblong apertures in order to facilitate the passing of the elongated prismatic crystals. Whenever possible, each size fraction was further divided by magnetic separation using the modified Frantz isodynamic separator. The final purification and the concentration of metamict crystals were achieved by hand-picking.

Apatite was concentrated from two samples by density separation in an overflow centrifuge. As most grains were broken during the crushing, no size fractions were made.

Chemical decomposition and separation of U and Pb were essentially according to the method described by Krogh (1973). The lead was purified by anodic deposition (Arden & Gale 1974). For further details, see Wielens et al. (1979).

The isotopic compositions were determined on a computer-controlled Teledyne SS-1290 mass-spectrometer with Faraday cage collector and digital output. Lead was mounted as nitrate on a single zone-refined Re filament with silica-gel and phosphoric acid, following the procedures described by Barnes et al. (1973). The typical sample load was about 0.5 μg. For the analysis of uranium, samples of about 0.5 μg uranium nitrate were loaded on the two zone-refined Re side filaments of a triple filament source. The isotopic composition of the spiked U samples was determined using the 'low-temperature' technique described by Shields (1966). The correction factors for mass fractionation are 0.15% per mass unit for uranium and 0.10% per mass unit for lead. These factors were obtained from the isotope composition measured for NBS uranium and lead standards; the main parameters responsible for isotope fractionation were kept constant for both standards and samples.

The combined effect of weighing errors, isotope ratio uncertainties and the error enlargement associated with isotope dilution analysis is estimated at 1%. Laboratory procedure blanks range from 1.5 to 3.6 ng for lead and are less than 0.2 ng for uranium. The aliquots processed for analysis are rather small (less than 20 mg), so inhomogeneities between the zircon crystals may cause notable differences in the repeats. When two aliquots of the same zircon fraction were analysed, these are therefore treated as different samples.

As the data-points in the concordia plot have correlated errors, the 'uncertainty area'

(corresponding to a 95% confidence region) around a point is represented as an ellipse. The discordia lines were calculated according to York (1969), assigning a correlation coefficient to each data-point and a weight to each coordinate. For the calculation of the correlation coefficients, the variances, the covariances and the error ellipses, see Boelrijk et al. (1979a, 1979b) and Kuijper (1979). The weights were taken as the reciprocal of the variances. For the calculation of the errors in the U–P discordia ages (1σ) both the standard deviation of the discordia slope and the systematic errors due to the spike calibration were taken into account.

5.2. Rb–Sr ANALYSIS

Pulverized whole-rock samples were analysed for their Rb and Sr contents and Rb/Sr ratios by X-ray fluorescence spectrometry, using a Philips PW 1450/AHP automatic spectrometer (pressed powder pellets; mass absorption corrections for both sample and external standard based upon the Compton scattering of the Mo–Kα beam (Verdurmen 1977). For the biotites, the Rb and Sr contents were determined by mass-spectrometric isotope dilution. Sr isotope compositions were determined directly on unspiked Sr for wholerocks and calculated from the isotope dilution runs for the biotites. All isotope measurements were made on a computer-controlled Varian CH5 mass-spectrometer with Faraday cage collector and digital output. The analytical accuracies are estimated at 1% for XRF Rb/Sr, 1% for isotope dilution Rb and Sr, and 0.05% for $^{87}Sr/^{86}Sr$. These overall limits of relative error are the sum of the known sources of possible systematic error and the precision (2σ) of the total analytical procedures.

Best-fit lines through the suites of Rb–Sr data were calculated by means of a least-squares regression analysis according to York (1966, 1967). The values of the Mean Squares Weighted Deviation (MSWD) were calculated according to McIntyre et al. (1966).

5.3. K–Ar ANALYSIS

The K contents were determined by flame photometry with a lithium internal standard and caesium chloride-aluminum nitrate buffer. Argon was extracted in a bakeable glass vacuum apparatus and determined by isotope dilution techniques under static conditions in a Reynolds-type mass-spectrometer. The accuracies are estimated at 1% for K and 2% for Ar.

5.4. CONSTANTS

All age calcultions are based upon the following constants (IUGS recommended values):
for uranium: $\lambda(^{238}U) = 1.55125\times 10^{-10}a^{-1}$, $\lambda(^{235}U) = 9.8485\times10^{-10}a^{-1}$, and atomic ratio $^{238}U/^{235}U = 137.88$;
for rubidium: $\lambda(^{87}Rb) = 1.42\times10^{-11}a^{-1}$;
for potassium: $\lambda e(^{40}K = 0.581\times10^{-10}a^{-1}$, $\lambda\beta(^{40}K) = 4.962\times10^{-10}a^{-1}$, and abundance $^{40}K = 0.01167$ atom percent total K.
For modern lead the composition of 'average modern lead' is taken: $\alpha = 18.700$, $\beta = 15.628$ and $\gamma = 38.630$ (Stacey & Kramers 1975). Lead isotopic ratios were corrected for procedure blanks assuming a modern lead composition, and for initial lead using a backward extrapolation from the modern lead with $\mu = 9.74$ and $W = 36.84$.

Where necessary, all ages quoted from literature have been recalculated with the above constants.

6. Zircon U-Pb systems

6.1. SAMPLES

Zircon U–Pb investigations were made on three augen gneisses (Rog 276, 279 and 298), two pyroxene syenites (Rog 283 and 285) and one garnetiferous migmatite (Rog 293). The locations are shown on the map of Fig. 1. The investigated samples are:

Rog 276 – a medium-grained, leucocratic quartz-monzonoritic augen gneiss;

Table 1. U–Pb data of the investigated Zircons and Apatites*

Sample Number and Fraction	Weight in mg (unspiked/spiked)	$^{204}Pb/^{205}Pb$ ($\times 10^4$)	$^{207}Pb/^{206}Pb$	$^{208}Pb/^{206}Pb$	$^{206}Pb/^{238}U$	$^{207}Pb/^{235}U$	Pb(ppm)	U(ppm)
Augen gneisses								
Rog 276								
A 20–30 μm	14.5 / 8.2	1.3	0.07362	0.1540	0.1487	1.471	111	706
B 50–60 μm	9.1 / 11.9	2.1	0.07482	0.1407	0.1514	1.499	119	750
C 70–90 μm	11.2 / 11.1	1.8	0.07502	0.1388	0.1544	1.541	117	720
D 110–130 μm	8.1 / 11.0	1.7	0.07482	0.1367	0.1578	1.576	98.7	598
Rog 279								
A 20–30 μm	7.5 / 5.1	6.1	0.08108	0.4144	0.1509	1.507	132	672
B 30–40 μm	7.9 / 8.3	6.0	0.08101	0.1838	0.1488	1.487	113	688
C 30–40 μm	15.8 / 12.1	3.5	0.07731	0.1681	0.1492	1.488	108	670
D 60–70 μm	14.7 / 12.3	5.1	0.07965	0.1561	0.1470	1.465	110	695
E 90–110 μm	14.1 / 12.2	9.4	0.08480	0.1609	0.1354	1.333	127	859
F +160 μm	16.0 / 13.2	21	0.1006	0.1847	0.1265	1.224	190	1303
Rog 298								
A 20–30 μm NOMA	9.0 / 5.5	14	0.09100	0.1432	0.1324	1.290	161	1114
Bm 20–30 μm MAG	2.7 / 4.2	28	0.1100	0.2146	0.1203	1.159	178	1234
C 50–60 μm NOMA	6.7 / 6.0	13	0.08915	0.1333	0.1330	1.300	159	1112
Dm 50–60 μm MAG	3.8 / 1.9	16	0.09342	0.1759	0.1251	1.214	171	1215
E 70–90 μm NOMA	8.0 / 3.2	18	0.09700	0.1525	0.1326	1.297	164	1111
Fm 70–90 μm MAG	8.5 / 4.2	12	0.08851	0.1333	0.1298	1.268	171	1221
Gm +90 μm MAG	8.4 / 8.0	22	0.1033	0.1696	0.1344	1.330	181	1183
H +160 μm NOMA	3.1 / 3.5	25	0.1066	0.1673	0.1333	1.309	190	1242
Apatites								
Rog 276	222 / 137	190	0.3453	1.060	0.1841	1.934	9.1	15.9
Rog 279	119 / 112	200	0.3522	1.042	0.1105	1.013	8.4	23.5

continued

Rog 279 – a slightly lineated, medium-grained, mesocratic biotite-amphibole-pyroxene augen gneiss;

Rog 298 – a medium-grained, leucocratic augen gneiss;

Rog 283 – a medium-grained, leucocratic, massive and homogeneous pyroxene-olivine-quartz monzonite;

Rog 285 – a medium-grained, mesocratic and distinctly lineated pyroxene-olivine-quartz syenite, containing small bands of mafic minerals;

Rog 293 – a fine-grained, leucocratic and slightly lineated quartz-rich garnet-spinel-bearing rock of granitic composition (garnetiferous migmatite).

A study of the morphology by Wielens (1979) revealed that all zircons show rounding and that many contain cores. Wielens concluded that the rounding of the zircon crystals was caused by metamorphic processes. The zircons from the garnetiferous migmatites show very little elongation and have gone through a sedimentary cycle. Those from the other rocks are elongated, suggesting an igneous origin.

6.2. RESULTS AND DISCUSSION

The analytical U–Pb data of the six investigated suites of zircons and two

Table 1. continuation

Sample Number and Fraction	Weight in mg (unspiked/spiked)	$^{204}Pb/^{206}Pb$ ($\times 10^4$)	$^{207}Pb/^{206}Pb$	$^{208}Pb/^{206}Pb$	$^{206}Pb/^{238}U$	$^{207}Pb/^{235}U$	Pb(ppm)	U(ppm)
Gloppurdi and Botnavatn igneous complexes								
Rog 283								
A 20–30 μm	7.5 / 9.6	2.5	0.07729	0.07950	0.1645	1.672	97.9	595
B 40–50 μm	8.5 / 9.5	0.9	0.07617	0.07875	0.1666	1.720	95.9	578
C 70–90 μm	8.6 / 10.6	0.8	0.07720	0.08194	0.1745	1.829	88.4	507
D 110–130 μm	13.3 / 10.3	1.3	0.07783	0.08298	0.1760	1.845	84.8	481
E 110–130 μm NOME	1.6 / 0.8	8.8	0.08934	0.1191	0.1783	1.889	65.4	347
F 110–130 μm HAME	1.3 / 0.7	2.3	0.07691	0.07513	0.1454	1.476	132	915
G +160 μm	9.1 / 7.2	1.2	0.07757	0.08022	0.1749	1.831	81.1	464
Rog 285								
A 20–30 μm	7.5 / 6.7	1.6	0.07673	0.08633	0.1677	1.721	62.6	372
B 30–40 μm	8.0 / 12.1	2.0	0.07730	0.08778	0.1688	1.733	60.8	358
C 40–50 μm	9.5 / 8.1	2.0	0.07726	0.08725	0.1703	1.748	67.8	396
D 50–60 μm	8.6 / 7.5	1.7	0.07652	0.08369	0.1708	1.746	67.6	396
E 50–60 μm	10.2 / 11.2	1.5	0.07663	0.08564	0.1710	1.756	65.6	383
F 70–90 μm	9.0 / 8.3	5.1	0.08209	0.09876	0.1741	1.798	66.7	374
G 90–110 μm	7.2 / 8.7	1.6	0.07693	0.08615	0.1730	1.780	64.6	372
Garnetiferous migmatites								
Rog 293								
A 20–30 μm	7.7 / 9.6	4.1	0.07851	1.0048	0.1684	1.688	207	680
B 40–50 μm	10.0 / 13.2	4.0	0.07867	0.1527	0.1633	1.642	119	683
C 50–60 μm	9.7 / 7.9	1.4	0.07622	0.6500	0.1711	1.751	182	711
D 60–70 μm	10.9 / 7.9	2.8	0.07733	0.2253	0.1677	1.696	132	698
E 70–90 μm	7.2 / 11.3	12	0.09025	0.3255	0.1740	1.756	154	711
F 90–110 μm NOME	1.1 / 0.6	9.1	0.08572	0.1344	0.1653	1.657	112	636
G 90–110 μm HAME	2.9 / 1.5	6.5	0.08137	0.8710	0.1479	1.471	172	1141
H 90–110 μm META	1.2 / 0.6	26	0.1052	0.1299	0.1151	1.081	284	2210
I 130–160 μm NOME	9.7 / 6.2	1.4	0.07444	0.1556	0.1681	1.679	139	779
J +160 μm META	3.5 / 3.1	5.7	0.08054	0.1054	0.1290	1.288	224	1682

* Column 1: HAME, partially metamict; MAG, magnetic; META, metamict; NOMA, non-magnetic; NOME, non-metamict; capital characters correspond with capital characters in Figs 2 through 7. Column 2: sample weight in milligrams for unspiked and spiked aliquots. Columns 3 through 5: measured $^{204}Pb/^{206}Pb$, $^{207}Pb/^{206}Pb$ and $^{208}Pb/^{206}Pb$ ratios. Columns 6 and 7: ratios radiogenic $^{206}Pb/^{238}U$ and $^{207}Pb/^{235}U$, after correction for the blank (assumed composition of modern lead: $^{206}Pb/^{204}Pb = 18.700$, $^{207}Pb/^{204}Pb = 15.628$, $^{208}Pb/^{204}Pb = 38.630$). Columns 8 and 9: total lead and uranium content.

apatites are given in Table 1. For each suite the data are plotted in a concordia diagram (Figs. 2–7).

6.2.a. THE AUGEN GNEISSES

Eighteen U–Pb analyses of zircon fractions are reported for the three augen gneiss samples. For sample Rog 276 four data-points were obtained from four size fractions. Of sample Rog 279 five size fractions were studied; two aliquots from one fraction were analysed separately, so six data-points were obtained. The five size fractions of sample Rog 298 were further divided into four magnetic and four non-magnetic fractions, producing eight data-points. The zircons of the magnetic fractions differ from the non-magnetic fractions in being slightly more metamict, but no other differences are apparent.

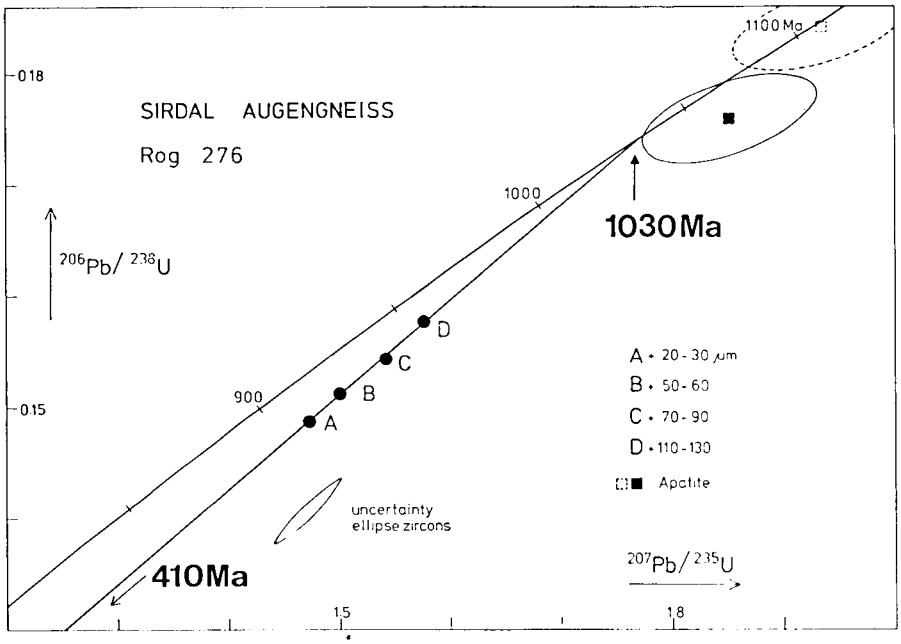

Fig. 2. Concordia diagram and U–Pb isotopic relationships of the zircon fractions and the apatite of augen gneiss Rog 276. The apatite was not included in the calculation of the regression line. The dashed and solid square and ellipse represent the extreme cases when all common lead is taken as initial lead and 'average modern lead', respectively.

The results are plotted in Figs. 2, 3 and 4. For each suite of zircons the data-points are discordant and show a linear correlation. The upper and lower intercepts are $1030 \pm {}^{35}_{30}$ Ma and 410 ± 90 Ma for Rog 276, $1045 \pm {}^{30}_{25}$ Ma and 350 ± 40 Ma for Rog 279, and $1030 \pm {}^{45}_{40}$ Ma and $310 \pm {}^{80}_{90}$ Ma for Rog 298. All three suites of zircons from the augen gneisses thus yield upper intercept ages between about 1030 and 1045 Ma, which may be taken as registering the complete expulsion of radiogenic lead during the highest-grade phase of Sveconorwegian metamorphism, M2. There appears to be no difference between zircons from amphibolite facies rocks and those from granulite facies rocks with regard to their U–Pb systematics. The lower intercepts of the three suites of zircons correspond to ages between about 410 and 310 Ma.

The data-points of the apatites have a large uncertainty ellipse because of their high $^{204}Pb/^{206}Pb$ ratio, a phenomenon possibly resulting from the analytical procedure: the 'acid wash' to remove surface contamination could not be applied. If all ^{204}Pb is taken to represent 'initial lead', the resulting data-points differ from those obtained when the common lead is assumed to have the composition of 'average modern lead' (Figs 2 and 3). For Rog 276 the resulting two data-points are significantly different, but in the case of Rog 279 the uncertainty ellipses overlap. It is possible, however, that the common lead in the apatite has a composition considerably different from 'initial lead' or

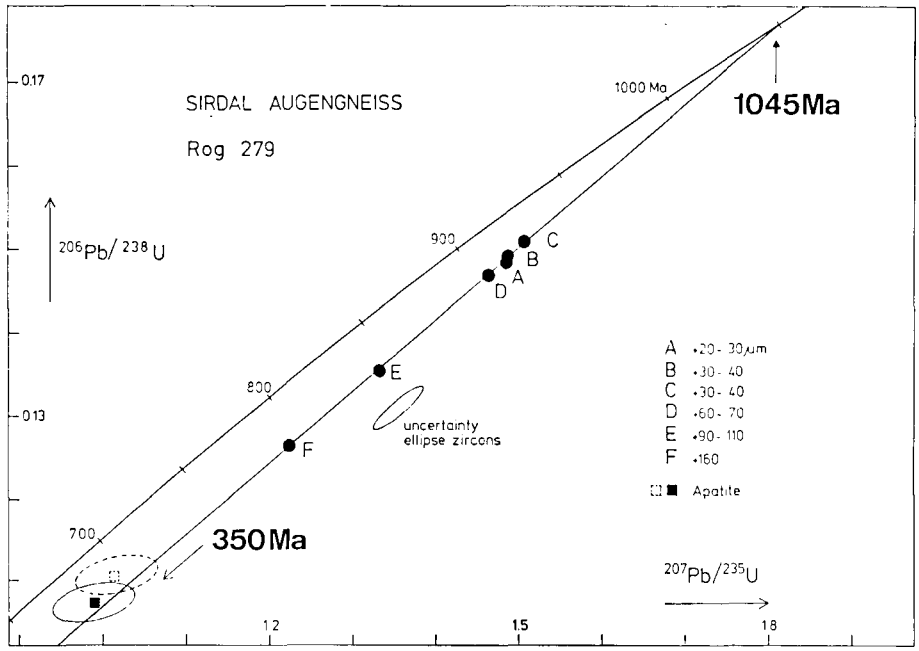

Fig. 3. Concordia diagram and U–Pb isotopic relationships of the zircon size fractions and the apatite of augen gneiss Rog. 279. The apatite was not included in the calculation of the regression line. The dashed and solid square and ellipse represent the extreme cases when all common lead is taken as initial lead and 'average modern lead', respectively.

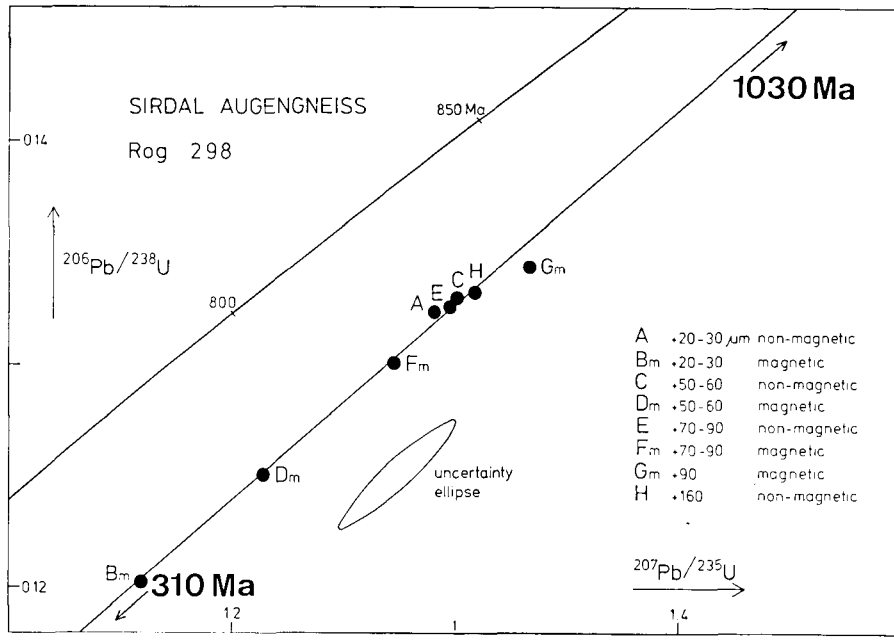

Fig. 4. Concordia diagram and U–Pb isotopic relationships of the zircon size fractions (split into magnetic and non-magnetic portions) of augen gneiss Rog 298.

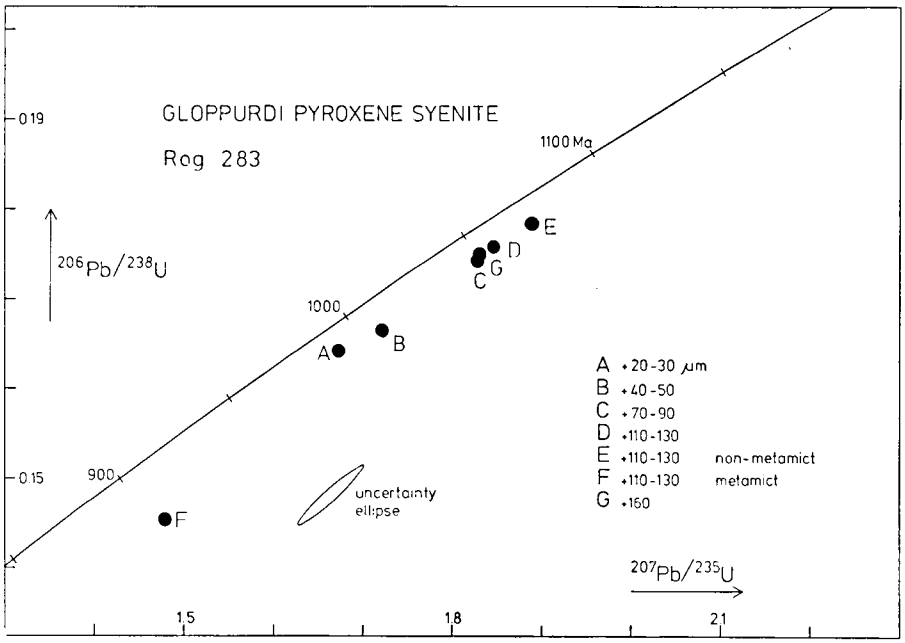

Fig. 5. Concordia diagram and U–Pb isotopic relationships of the zircon size fractions (one fraction split into metamict and non-metamict portions) of pyroxene syenite Rog 283.

'average modern lead'. If all ^{204}Pb is taken to represent contamination with 'average modern lead', the apatite of Rog 276 plots within the limits of error at the upper intercept of the discordia through the zircon data-points. This suggests that the composition of the common lead in the apatite approaches that of 'average modern lead'. In Rog 279 both apatite data-points are clearly discordant, an uncommon feature for this mineral, but they do fit the discordia through the zircon data-points.

6.2.b. THE PYROXENE SYENITES

A total of fourteen U–Pb analyses is reported of zircon fractions from the two pyroxene syenite samples. Of sample Rog 283 from the Gloppurdi igneous complex five size fractions were investigated. Part of one fraction (110–130 μm) was further divided into two portions, one consisting of mainly metamict and the other of mainly non-metamict crystals; both portions were analysed along with the undivided part of the fraction. Six size fractions were investigated of sample Rog 285 from the Botnavatn igneous complex; one of them was split into two aliquots and each analysed separately.

The results are plotted in Figs 5 and 6. For sample Rog 285 the data-points define a discordia with upper and lower intercepts at $1070 \pm {}^{30}_{25}$ and 365 ± 160 Ma. The scatter of the data-points of Rog 283 is too large to allow a discordia calculation through all points; this scatter may be ascribed to relics with a U–Pb history older than about 1050 Ma. The age of Sveconorwegian recrystallization of these zircons might be approached most nearly

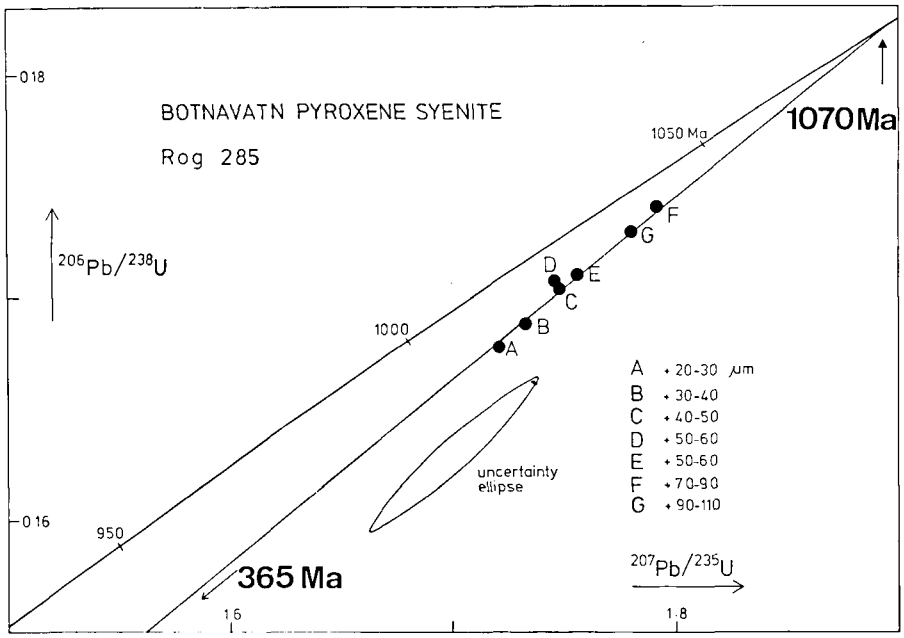

Fig. 6. Concordia diagram and U–Pb isotopic relationships of the zircon size fractions of pyroxene syenite Rog 285.

by a line through the finest fraction (20–30 µm) and the 365 Ma point at the concordia, producing an upper intercept at about 1055 Ma. The upper intercept age of 1070 Ma of sample Rog 285, on the other hand, can be interpreted as approaching the time of (nearly) complete loss of older radiogenic lead during the Sveconorwegian metamorphism.

6.2.c. THE GARNETIFEROUS MIGMATITE

The data-points of the ten investigated fractions of sample Rog 293 come from seven size fractions. Two of them were further divided, one (90–110 µm) into three portions consisting of non-metamict, partially metamict and metamict crystals, the other into a metamict and a non-metamict portion. The ten data-points scatter and do not show a linear correlation (Fig. 7). Except for the three metamict and partly metamict portions, the other data-points are roughly concordant at about 1000 Ma.

The scatter of the data-points can be explained in terms of the sedimentary derivation of the zircons. Detrital zircons may vary in age, in radiogenic lead content and in mineralogical characteristics, leading to a different response of the U–Pb systems to the Sveconorwegian metamorphism. Some types of zircon may have been fully reset, whereas others retained some of the previously accumulated radiogenic lead. An inheritance of some old radiogenic lead in the zircons is supported by the Rb–Sr systematics of a suite of samples from this unit, which indicates a prolonged pre-metamorphic Rb–Sr history (chapter 7.2).

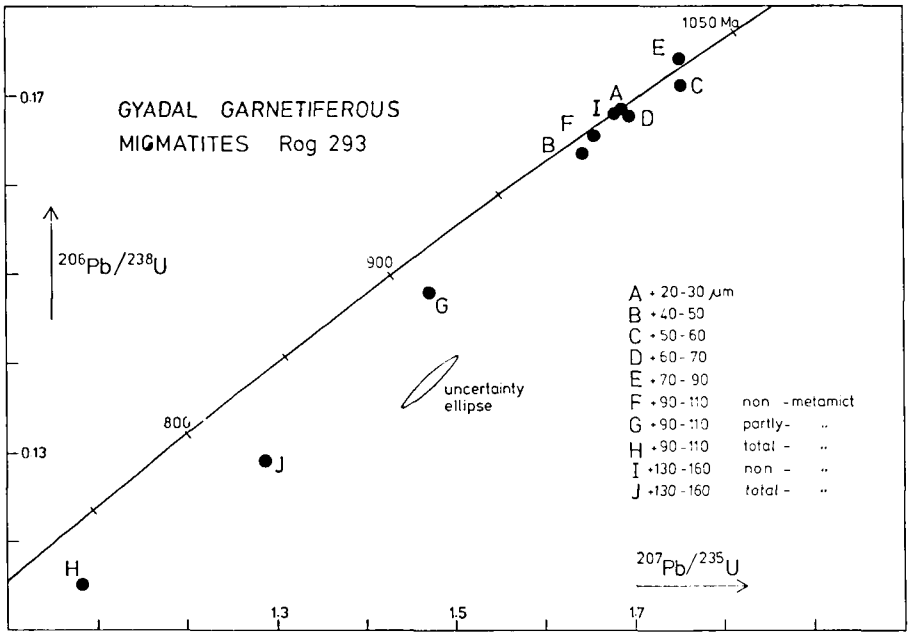

Fig. 7. Concordia diagram and U–Pb isotopic relationships of the zircon size fractions (two fractions split into metamict, partly metamict and non-metamict portions) from garnetiferous migmatite Rog 293.

6.3. THE LOWER INTERCEPT AGES

The zircons from the three augen gneisses and one pyroxene syenite yield discordia trajectories with lower intercepts between about 410 and 310 Ma. Similar lower intercept ages have also been reported for zircons from different locations elsewhere in the basement complex of southern Norway and southwestern Sweden (Swainbank 1965), and from the basement below the Jotunnappe complex in the Caledonian belt (Corfu 1978, 1979). Such persistence of Paleozoic ages in Precambrian rocks situated along the front of the Caledonian nappe system or within the Caledonides suggests a geological significance. In the area under discussion the biotite K–Ar and Rb–Sr systems do not show any resetting in relation to Caledonian orogenesis (Versteeve 1975, Verschure et al. 1979, 1980, this study), so the temperature in the rocks remained below the temperature at which biotite opens to Rb–Sr and K–Ar. On the other hand, the phase of incipient very-low-grade metamorphism, M4, indicated by the local occurrence of minerals of the pumpellyite-prenite facies, could very well reflect the influence of the nearby belt of Caledonian orogenesis. This is supported by the Caledonian ages determined on secondary biotites in an approximately 10 km-wide zone along the front of the Caledonian nappe system north of the map area of Fig. 1 (Verschure et al. 1979, 1980). The lower intercepts of the discordia trajectories are thus compatible with episodic loss of radiogenic lead due to a moderate increase in temperature in the Shield rocks in front of the belt of Caledonian orogenesis, and/or with Goldich & Mudrey's

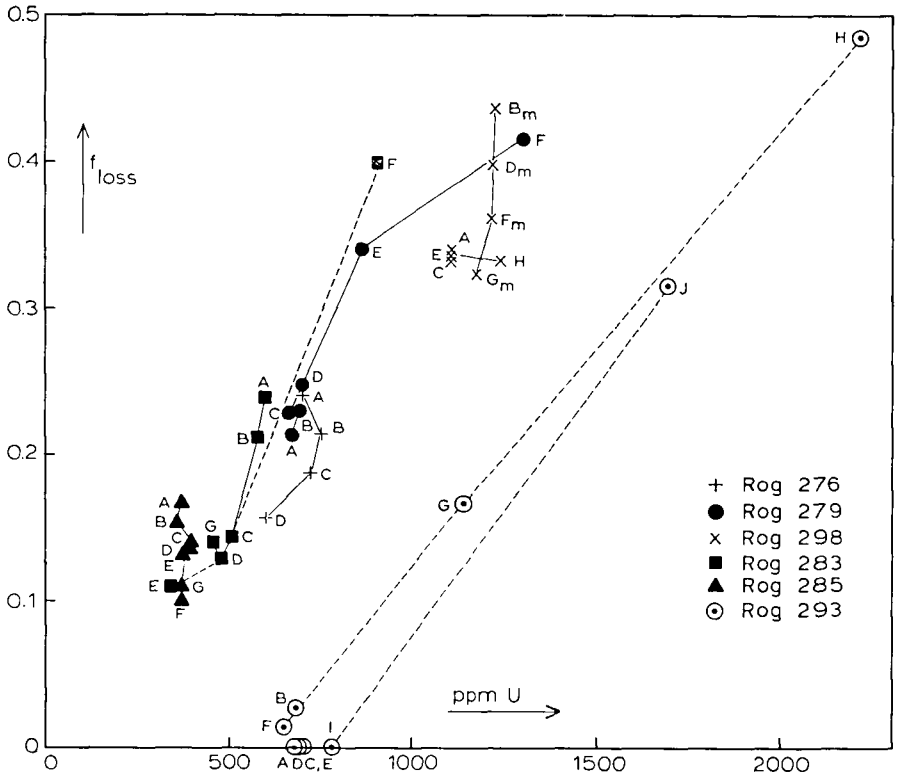

Fig. 8. Plot of fractional loss or radiogenic lead, f_{loss}, against the uranium content for each of the investigated zircon fractions. For each suite of zircons the full lines connect the data-points in order of crystal sice. The dashed lines connect the data-points in order of degree of migmatization. The letters correspond to the letters used for the different fractions in Table 1 and Figs. 2 to 7. For further discussion, see text.

(1972) uplift/dilatance model for lead from zircon in relation to uplift and erosion of the crustal block after the termination of the Caledonian orogeny. Many lower intercept ages lie in fact below the known range of Caledonian ages; this is explained by Corfu (1979) in terms of the time needed for thermal equilibration between the overthrust nappe and the cold basement.

6.4. DEGREE OF LEAD LOSS

There generally is a strong correlation between uranium content of zircons on the one hand and grain size, metamictization and magnetic susceptibility on the other: the uranium content usually increases with decreasing grain size, increasing metamictization and increasing magnetic susceptibility. It is commonly observed that the degree of radiogenic lead loss is related in the same way to these parameters. According to Sommerauer (1976) the metamictization of zircons is essentially restricted to the so-called Z_m-phase, the physico-chemically unstable phase where all foreign elements, including uranium, are concentrated. This phase may easily lose its radiogenic lead (and other foreign

elements) under conditions of moderate temperature (already at 200°C), alteration and/or pressure release during uplift.

In order to visualize the relationship between lead loss and the relevant parameters more clearly than in concordia-discordia plots of the investigated suites of zircons, the uranium content is plotted against the fractional lead loss for each zircon fraction in Fig. 8. The fractional lead loss, f_{loss}, is defined as the fraction of radiogenic lead lost during the lead-loss event. The fraction is calculated as $f_{loss} = (y_u - y_z)/(y_u - y_l)$, where y_z is the $^{206}Pb/^{238}U$ ratio of the zircon after correction for blank and initial lead, and y_u and y_l are the $^{206}Pb/^{238}U$ ratios corresponding to the upper and lower intercepts in the concordia plot. It is assumed in this calculation that no loss of uranium has taken place. Lines are drawn connecting the data-points of each suite of zircons in order of the crystal size.

From the plot in Fig. 8 it is clear that there is an inverse correlation between the degree of lead loss and the grain size for the suites Rog 276 (augen gneiss) and 285 (pyroxene syenite), where all fractions have about the same uranium content. For Rog 279 (augen gneiss) the degree of lead loss is proportional to the grain size, but here the uranium content also increases with the grain size. Among the zircon fractions of Rog 298 (augen gneiss) two groups can be distinguished: for each size fraction the magnetic portion suffered a somewhat higher lead loss than the non-magnetic zircons, in accordance with a somewhat higher uranium content. All fractions of this suite have uranium contents between about 1110 and 1250 ppm. The magnetic portions show an increasing lead loss with decreasing grain size, whereas the fractional loss from the non-magnetic zircons is about the same for all size fractions. For Rog 283 (pyroxene syenite) the fractional lead loss increases both with increasing uranium content and with decreasing grain size. The metamict (E) and non-metamict (F) portions of the 110–130 μm size fraction (D) of this suite display an increasing fractional lead loss with increasing uranium content and increasing metamictization.

The suites of zircons from the five magmatic rocks display a roughly linear trend in the diagram. They confirm the proportionality of the fractional radiogenic lead loss with the uranium content. The similar behaviour of the magmatic zircons may be attributed to the fact that they have about the same history: (re)crystallization and nearly complete lead loss about 1050 Ma ago, followed by an event of partial lead loss about 400 Ma ago.

The only concordant or nearly concordant zircons in this study are seven fractions from the garnetiferous migmatite Rog 293, all with uranium contents between about 600 and 800 ppm. They cluster around the upper intercept irrespective of the crystal size. The metamict (H), partial metamict (G) and non-metamict (F) portions of the 90–110 μm size fraction of this suite display an increasing fractional lead loss with increasing uranium content and increasing metamictization. The same holds for the non-metamict (I) and metamict (J) portions of the 130–160 μm size fraction. The fact that the zircons of this suite have gone through a sedimentary cycle (Wielens 1979)

could be an explanation for the near concordance of seven of the ten zircon fractions. This is in accordance with Sommerauer's (1976) view that sedimentary-derived zircons consist of a relatively high proportion of the non-metamict, physico-chemically stable Z_k-zircon.

6.5. COMPARISON WITH OTHER ZIRCON AGES REPORTED FROM THE SIRDAL–ØRSDAL AREA

All previously reported zircon U–Pb ages from the high-grade metamorphic basement in the Sirdal–Ørsdal area were obtained in the Z.W.O. Laboratorium voor Isotopen-Geologie, Amsterdam (Versteeve 1975), and by the Brussels group (Pasteels & Michot 1975). Versteeve reported upper and lower intercept ages of 1250 and 770 Ma for one suite of zircons from a charnockitic migmatite in Drangsdalen. He interpreted the age of 1250 Ma as a true age, recording the early Sveconorwegian phase of upper amphibolite facies metamorphism. In view of the new zircon data, however, this age is now interpreted in terms of a two-stage isotopic disturbance model, i.e. a first stage about 1050 Ma ago with incomplete loss of the previously accumulated radiogenic lead, and a second stage in (post-)Caledonian time. The upper and lower intercepts of the Drangsdalen suite of zircons should then have no geochronological significance. An old radiogenic lead component should thus have been retained in the crystals during the Sveconorwegian metamorphism, but no conclusions are possible regarding the age of this component.

The Brussels group reported zircon ages of augen gneisses, garnetiferous migmatites and granitic migmatites. Most of these ages are based upon two or three fractions; any scatter in the data-points is thus not revealed, so some caution should be exercised in using the ages. Of the four augen gneisses, two have zircons with upper intercept ages in the same Sveconorwegian range as displayed by the augen gneisses investigated in this study. The other two augen gneisses, from outside the map area of Fig. 1, yield somewhat younger ages of about 900 to 950 Ma. A few samples from the garnetiferous migmatites and the granitic migmatites produce higher upper intercept ages: about 1500 Ma and 1200 Ma. It is difficult to judge whether they document geological events. Similar ages have also been reported for other isotopic systems from the area (Pasteels & Michot 1975, Versteeve 1975) and from elsewhere in the Baltic Shield (Magnusson 1965, Welin 1974, Skiöld 1976, Welin & Gorbatschev 1978a, 1978b, 1978c, Schaerer 1978, Corfu 1978, 1979, Daly et al. 1979) so they may record events of widespread metamorphism: a pre-Sveconorwegian phase, M0, and the first Sveconorwegian phase under upper-amphibolite facies conditions, M1. However, the high intercept ages reported by the Brussels group could also be interpreted, at least in part, as cases of inherited old radiogenic lead due to an incomplete expulsion of lead from the crystals during the Sveconorwegian metamorphism; in that case they should not document geological meaningful ages. This interpretation appears to be the more feasible when the lower intercepts correspond to geologically improbable ages.

6.6. CONCLUSIONS REGARDING THE ZIRCON U–Pb SYSTEMS IN THE SIRDAL–ØRSDAL AREA

The U–Pb systematics of the zircons in the high-grade metamorphic Precambrian of the Sirdal—Ørsdal area may be interpreted in terms of a two-stage episodic lead-loss model, as follows:

1. During the phase of highest-grade metamorphism about 1050 Ma ago (M2) older zircons lost (nearly) all of their previously accumulated radiogenic lead.
2. Some suites of zircons appear to have retained part of the old radiogenic lead during the metamorphism. In some cases this leads to more or less linear arrangements in the concordia plot with upper and lower intercepts without geochronological meaning.
3. No conclusions are possible regarding the age of the older zircon component.
4. Suites of zircons which lost all of their previously accumulated radiogenic lead define discordia trajectories with upper intercepts between about 1070 and 1030 Ma and lower intercepts ranging from about 410 to 310 Ma.
5. The lower intercept ages of about 410–310 Ma are interpreted as recording radiogenic lead loss in relation to the nearby belt of Caledonian orogenesis or post-orogenic uplift under conditions of relatively low ambient temperature (no resetting is shown by the biotite K–Ar and Rb–Sr systems). This episode may be related to the local retrograde phase of incipient pumpellyite-prehnite facies metamorphism (M4), and the development of secondary biotite with an age of about 400 Ma in a narrow zone along the Caledonides north of the map area of Fig. 1.

7. Whole-rock Rb-Sr systems

7.1. SAMPLES

In this study Rb–Sr whole-rock analyses have been made of three suites of samples from the high-grade metamorphic basement (Fig. 1):

A – Eleven samples (Rog 3, 59, 60 and 180–187) from the band of garnetiferous migmatites south of Saetravatnet. All samples were taken from one quarry within a distance of some 20 m. The Rb–Sr data of three of them (Rog 3, 59 and 60) have already been published by Versteeve (1975).

B – Six samples (Rog 248, 251 and 254–257) of granitic migmatite near Sinnes, north of the map area of Fig. 1 (N.G.O. grid coordinates 3732–65314). The samples are slices sawn according to the compositional banding from a single specimen of banded rock.

C – Ten samples (Rog 258–267) of fine-grained granulitic gneiss from a location south of Store Myrvatnet. The samples come from a small area of about 2×2 m.

7.2. RESULTS AND DISCUSSION

The Rb–Sr data of the 27 whole-rock samples are given in Tables 2, 3 and 4.

Table 2. Rb–Sr whole-rock data garnetiferous migmatite, south of Sætravatn

Sample Nr.	Rb (ppm Wt)	Sr (ppm Wt)	Rb/Sr (Wt/Wt)	$^{87}Sr/^{86}Sr$	$^{87}Rb/^{86}Sr$
Rog 3*	216	95.5	2.260	0.8143	6.610
Rog 59*	320	237	1.355	0.7692	3.944
Rog 60*	140	288	0.4858	0.7284	1.410
Rog 180	153	360	0.4236	0.72375	1.227
Rog 181	263	154	1.703	0.79697	4.970
Rog 182	183	198	0.9234	0.75412	2.684
Rog 183	146	122	1.202	0.77970	3.502
Rog 184	162	158	1.024	0.76372	2.979
Rog 185	208	302	0.6898	0.74000	2.002
Rog 186	121	77.2	1.564	0.80424	4.568
Rog 187	280	183	1.530	0.77988	4.459

* Data published by Versteeve (1975).

Table 3. Rb–Sr whole-rock data slices of a banded sample of granitic migmatite, Sinnes

Sample Nr.	Rb (ppm Wt)	Sr (ppm Wt)	Rb/Sr (Wt/Wt)	$^{87}Sr/^{86}Sr$	$^{87}Rb/^{86}Sr$
Rog 248	278	313	0.8881	0.74413 0.74371	2.581
Rog 251	68.0	330	0.2064	0.71711 0.71686	0.5983
Rog 254	98.1	296	0.3320	0.72495 0.72470	0.9632
Rog 255	153	349	0.4368	0.72750 0.72812	1.267
Rog 256	379	252	1.509	0.76941 0.76919	4.397
Rog 257	27.4	265	0.1036	0.71486 0.71464	0.3003

For each suite the data are plotted in a $^{87}Sr/^{86}Sr$–$^{87}Rb/^{86}Sr$ diagram. None of the investigated suites of samples produces an isochron relationship. For the garnetiferous migmatites the data-points scatter within an envelope with upper and lower boundaries of about 1500 and 1100 Ma, respectively (Fig. 9). The suites of samples from the granitic migmatite and the granulitic gneisses show rough linear correlations. Regression analyses produce best-fit lines corresponding to an age of 931 ± 90 Ma (MSWD = 9.2) for the former (Fig. 10) and 1216 ± 90 Ma (MSWD = 23.0) for the latter (Fig. 11); the initial $^{87}Sr/^{86}Sr$ ratios are 0.711 ± 0.002 and 0.715 ± 0.017, respectively (all errors at 95% confidence level as computed from the scatter of the data about the regression line).

The Rb–Sr data of the three suites of samples indicate widespread migration of

Table 4. Rb–Sr whole-rock data granulitic gneisses south of Store Myrvatn

Sample Nr.	Rb (ppm Wt)	Sr (ppm Wt)	Rb/Sr (Wt/Wt)	$^{87}Sr/^{86}Sr$	$^{87}Rb/^{86}Sr$
Rog 258	430	40.1	10.74	1.2637	32.76
Rog 259	344	61.4	5.603	1.0031	16.68
Rog 260	456	38.1	11.97	1.3514	36.81
Rog 261	465	46.6	9.997	1.2372	30.43
Rog 262	251	76.5	3.280	0.89372	9.663
Rog 263	313	126	2.488	0.83919	7.291
Rog 264	364	126	2.889	0.85584	8.480
Rog 265	277	53.4	5.191	1.0088	15.46
Rog 266	360	58.9	6.119	1.0163	18.24
Rog 267	263	27.7	9.484	1.2207	28.83

Rb and/or Sr during the Sveconorwegian metamorphism, in accordance with the results obtained by Versteeve (1975). Although no complete Sr isotopic equilibration was attained, the granitic migmatite and the granulitic gneiss display a fairly large degree of homogenization through each suite of samples. They appear to approach linear arrangements of about 930 Ma and 1215 Ma, respectively. The age of about 930 Ma accords with the Sr isotopic equilibration ages of 930 ± 25 Ma and 980 ± 85 Ma reported from the area by Versteeve (1975); all these ages may be related to the last phase of Sveconorwegian high-grade metamorphism, M3. Provisionally, an age of about 950 Ma is therefore assigned to this phase of regional metamorphism. Whether the apparent higher age of the granulitic gneisses reflects the M1 phase of upper amphibolite facies metamorphism remains a matter of speculation. Both suites have fairly high initial $^{87}Sr/^{86}Sr$ ratios (about 0.711 and 0.715, respectively, suggesting a substantial pre-metamorphic Rb–Sr record.

The Rb–Sr systems of several garnetiferous migmatite samples record a prolonged pre-Sveconorwegian Rb–Sr history. The upper boundary line corresponds to an age of 1500 Ma; such an age has been reported from several places in S. W. Norway (chapter 6.5), but whether this line has any geochronological meaning (M0?) remains a matter of speculation.

8. AGE OF THE (QUARTZ-)MONZONITIC PHASE OF THE BJERKREIM–SOKNDAL LOPOLITH

The Rb–Sr whole-rock isochron ages of 842 ± 30 Ma and 857 ± 21 Ma determined by Versteeve (1975) and Pasteels et al. (1979), respectively, are too low when compared to the corresponding age of about 950 Ma measured on zircons (Pasteels et al. 1970, 1979) and hornblendes (this study). Versteeve based his calculation upon the analysis of 25 samples, collected all over the (quartz-)monzonitic phase of the lopolith. On the other hand, if only eight samples from within some 100 m along a fresh road cut (Rog 146 through 153, location D on the map of Fig. 1) are taken into account, a regression line can be calculated through seven samples of the same composition; sample Rog 147, a xenolith with a clearly different petrography (Dr. C. Maijer, pers. comm.

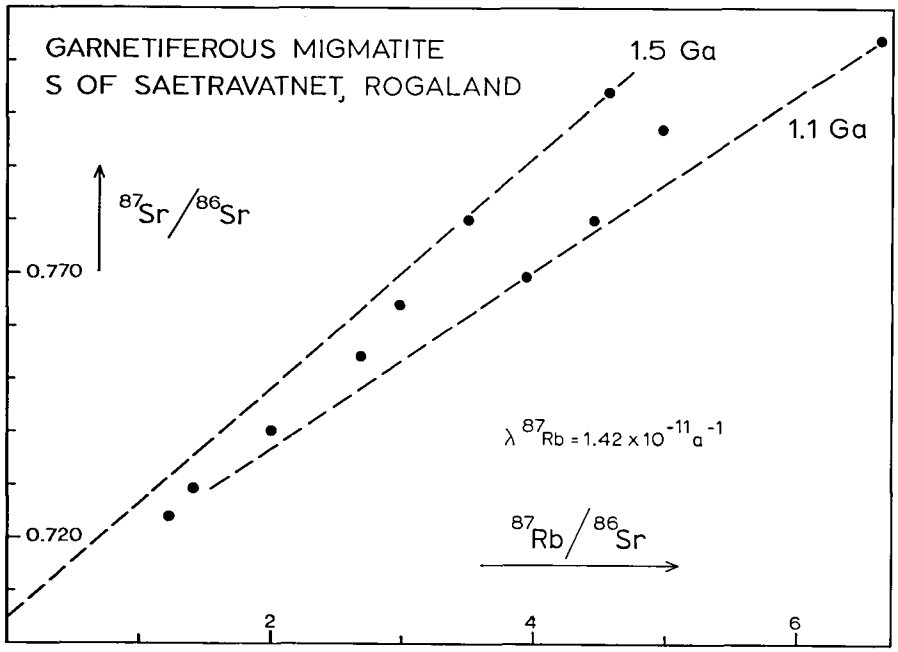

Fig. 9. Plot of Rb–Sr whole-rock data of the garnetiferous migmatites south of Sætravatnet (A on the map of Fig. 1).

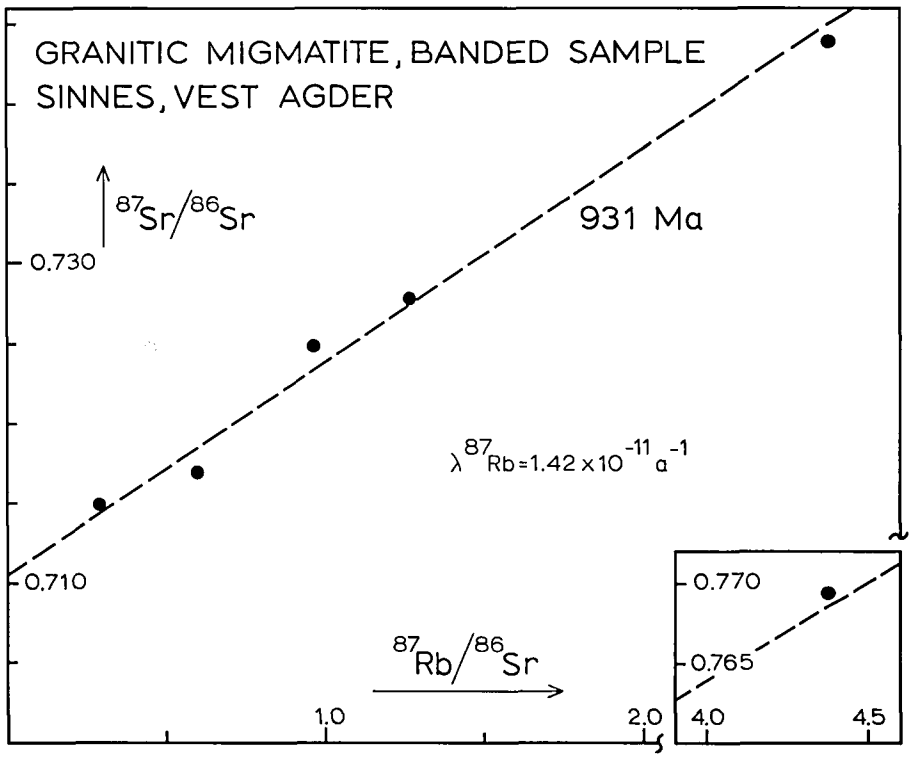

Fig. 10. Plot of the Rb–Sr whole-rock data of slices from a banded sample of granitic migmatite near Sinnes (location B, north of the map area of Fig. 1).

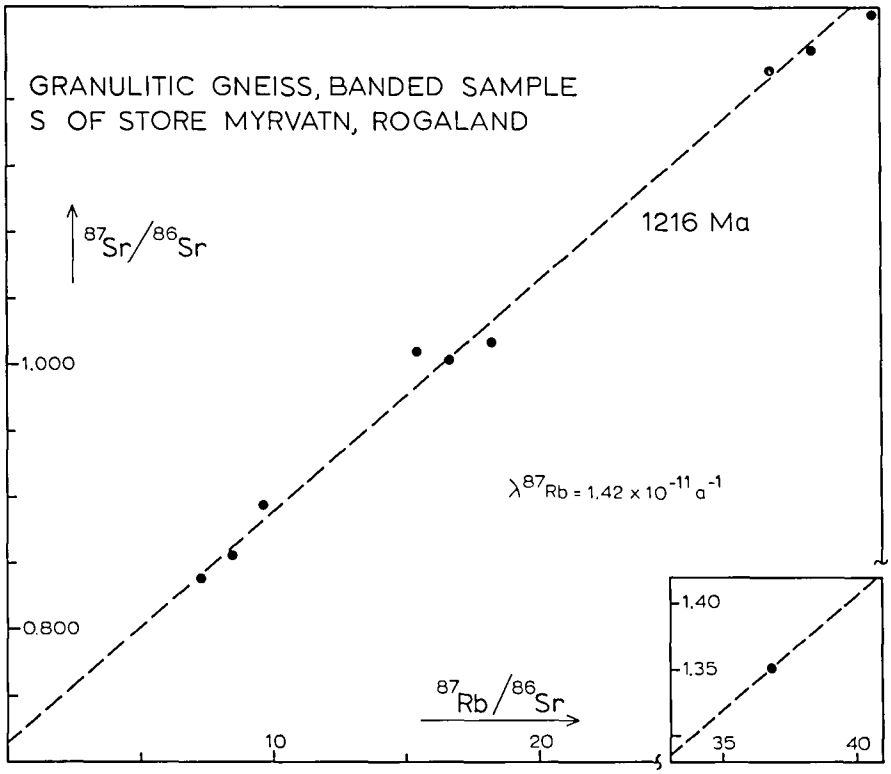

Fig. 11. Plot of the Rb–Sr whole-rock data of the fine-grained granulitic gneisses south of Store Myrvatn (C on the map of Fig. 1).

1979) was omitted. This results in an age of 928 ± 50 Ma with initial $^{87}Sr/^{86}Sr$ = 0.7075 ± 0.0028 (MSWD = 0.3: errors at 95% confidence level as computed from the scatter of the data about the regression line), in much better agreement with the age of about 950 Ma displayed by the zircon U–Pb systems. The isotopic ages presently available appear to indicate an intrusion age of about 950 Ma for this phase of the lopolith.

All whole-rock Rb–Sr, zircon U–Pb and hornblende K–Ar ages (chapter 9) fall within the interval of about 960–930 Ma. This suggests that within a relatively short time interval after the intrusion of the (quartz-)monzonitic phase the rocks cooled from the intrusion temperature of about 1000°C (chapter 2) to the blocking temperature of hornblende to K–Ar, 550–490°C (chapter 9.1). The initial $^{87}Sr/^{86}Sr$ ratio of 0.7075 indicated by the suite of seven samples agrees fairly well with the initial ratio of 0.7085 reported by Duchesne & Demaiffe (1978) for this part of the lopolith.

The apparently too low Rb–Sr ages obtained by Versteeve and Pasteels et al. may be explained by local Sr isotopic exchange between parts of the (quartz-) monzonitic magma and xenoliths (Hermans et al. 1975) already enriched in ^{87}Sr. Such a process is also suggested by the high initial $^{87}Sr/^{86}Sr$ ratios of the two 'isochrons', 0.7121 ± 0.0012 and 0.7107 ± 0.0004, respectively.

Table 5. Dated hornblendes from the Sirdal–Ørsdal area

Sample Nr.	Rock type and location (Fig. 1)
Rog 43	biotite amphibolite, SE of Moi
Rog 129	quartz–hornblende norite, SE of Moi
Rog 175	granitic migmatite, SE of Moi
Rog 242	augen gneiss, Øvre Sirdal
Rog 244	idem
Rog 252	granitic migmatite, Sinnes*
Rog 334	gabbroic sill cutting garnetiferous migmatite, North of Ørsdalsvatn
Rog 335	idem
Rog 336	charnockitic migmatite near the lopolith, immediately SE of anorthositic outlier, W of Lundevatnet
Rog 337	olivine amphibolite between anorthositic outlier and lopolith (border zone of lopolith), W of Moi
Rog 338	amphibole–ilmenite–apatite hypersthenite (phase A of lopolith), NE of Sokndal, W of Lundevatnet
Rog 339	biotite amphibolite, E of Tonstad
Rog 340	amphibole granite, top of lopolith, S of Teksevatnet (hornblende replaces pyroxene)
Rog 341	quartz norite from folded basic intrusion, SW of Tonstad
Rog 342	olivine–pyroxene hornblendite, immediately outside lopolith, W of Moi (pargasite)
Rog 343	schistose pyroxene–amphibole enderbite, NE of Tonstad
Rog 344	hornblendite, NW of Tonstad

* Location B, north of map area

9. Hornblende ages

K–Ar data and calculated ages are reported here of seventeen hornblendes, two from the lopolith (Rog 338 from the leuconoritic lower part and Rog 340 from the quartz-monzonitic upper part) and the other from various rocks in the high-grade metamorphic basement all over the Sirdal–Ørsdal area (Fig. 1 and Table 5; Dekker 1978). The data of three hornblendes (Rog 43, 129 and 175) are from Versteeve (1975).

9.1. RESULTS AND DISCUSSION

The analytical data and calculated K–Ar ages are given in Table 6. Except for sample Rog 43, all hornblende data lie between about 970 and 940 Ma, averaging 953 ± 10 Ma. This age is interpreted as a cooling age after the climax of the last phase of Sveconorwegian metamorphism, M3. From the consistence of hornblende ages throughout the area, both in the lopolith and in the high-grade metamorphic terrain, it is evident that the rocks exposed in the Sirdal–Ørsdal area have passed the blocking temperature at about the same time: this temperature can be taken at about 550–490 °C (Hart et al. 1968, Andriessen 1978). As an age of about 950 Ma is assigned to the M3 phase of metamorphism, the cooling from the climax of the lower granulite/upper amphibolite facies conditions to 550–490 °C must have been relatively fast.

The high age of hornblende Rog 43 probably represents a case of excess radiogenic Ar, an explanation supported by the likewise too high K–Ar age of

Table 6. K–Ar hornblende data and calculated ages

Sample Nr.	K (% Wt)	radiogenic ^{40}Ar (ppm Wt)	atmospheric ^{40}Ar (ppm Wt)	Calculated age (Ma)**
Rog 43*	1.33	0.148	5	
	1.32	0.158	3	
		0.152	7	1171
		0.152	6	
		0.151	2	
Rog 129*	1.33	0.118	4	
	1.33	0.114	4	
		0.111	27	942
		0.113	6	
		0.112	2	
Rog 175*	1.30	0.111	7	939
	1.29	0.110	2	
		0.111	2	
Rog 242	1.13	0.0984	2	956
	1.13	0.0990	2	
	1.14			
Rog 244	1.10	0.0947	2	963
	1.06	0.0956	2	
	1.08			
Rog 252	1.31	0.118	2	972
	1.31	0.115	3	
Rog 334	1.71	0.150	18	949
	1.71	0.146	13	
Rog 335	1.45	0.128	23	971
	1.45	0.130	12	
Rog 336	1.25	0.107	25	941
	1.25	0.108	13	
Rog 337	1.23	0.108	24	948
	1.24	0.107	16	
Rog 338	1.013	0.0871	20	959
	1.009	0.0901	13	
Rog 339	0.722	0.0639	14	964
	0.701	0.0618	21	
Rog 340	0.986	0.0867	14	951
	1.004	0.0858	23	
Rog 341	1.21	0.105	20	937
	1.21	0.101	13	
Rog 342	0.495	0.0439	20	963
	0.501	0.0439	13	
Rog 343	0.903	0.0767	14	937
	0.908	0.0774	25	
Rog 344	0.796	0.0701	15	956
	0.800	0.0693	20	

* Data published by Versteeve (1975).
** Error estimated at 3%, based upon estimated errors of 1% for K and 2% for Ar.

Table 7. Dated biotites from the Sirdal–Ørsdal area

Sample Nr.	Rock type and location (Fig. 1)
Rog 8	anorthosite, S of Heskestad (anorthositic outlier)
Rog 16	coarse-grained, gneissose granite SE of Sinnes*
Rog 18	augen gneiss, NW of Tonstad
Rog 24	pyroxene diorite, S of Tonstad (folded basic intrusion)
Rog 40	charnockitic migmatite, Virak on western shore Sirdalsvatn
Rog 43	biotite amphibolite, SE of Moi
Rog 74	charnockitic migmatite, Søyland
Rog 75	quartz–hypersthene diorite, Austrumdal
Rog 244	augen gneiss, north of Tonstad
Rog 248	granitic migmatite, Sinnes**

* North of map area (NGO grid coordinates 65282–3885)

** Location B, north of map area

the biotite from this sample (chapter 10.1). Versteeve's (1975) interpretation of this age as a 'relict age' of the older phase of upper amphibolite facies metamorphism about 1200 Ma ago (M1) has become improbable in view of the new hornblende data.

10. Biotite ages

K–Ar analyses were made of ten biotites from the Sirdal–Ørsdal area, one from the anorthositic outlier and the other from various rocks in the high-grade metamorphic basement all over the area (Table 7). Rb–Sr dates of eight of them have already been published by Versteeve (1975). The Rb–Sr date of biotite Rog 244 was obtained in this study.

10.1. RESULTS AND DISCUSSION

The analytical K–Ar data and calculated ages are listed in Table 8. Along with the K–Ar ages the Rb–Sr ages are given. For Rog 244 also the analytical Rb–Sr data are presented. Except for the higher K–Ar age of Rog 43, all biotite ages lie between about 900 and 850 Ma. The K–Ar age of 940 Ma of biotite Rog 43 probably represents a case of excess radiogenic Ar, in view of the corresponding Rb–Sr age of 878 Ma and the likewise too high K–Ar age measured on the hornblende from this rock (chapter 9.1). If ages of 950 Ma and 875 Ma are assumed for the hornblende and the biotite, respectively, both minerals appear to contain about the same amount of excess radiogenic Ar, about 25.10^{-6} cm^3 NTP/g.

The ages in the range from 900 to 850 Ma are interpreted as cooling ages, indicating that after the M3 phase of Sveconorwegian metamorphism the temperature in the rocks had decreased to the blocking temperature of biotite to Rb–Sr and K–Ar about 870 Ma ago. For this blocking temperature values of 300 ± 50°C (Jäger et al. 1967) and 360 to 400°C (Andriessen 1978)

Table 8. K–Ar biotite data and calculated K–Ar and Rb–Sr ages

Sample	K (% Wt)	radiogenic ^{40}Ar (ppm Wt)	atmospheric ^{40}Ar (% total ^{40}Ar)	K–Ar age*	Rb–Sr age**
Rog 8	6.00	0.459	21	867	895
	5.91				
Rog 16	6.42	0.489	17	857	853
	6.44				
Rog 18	5.63	0.426	16	854	858
	5.63				
Rog 24	7.75	0.609	11	878	894
	7.78				
Rog 40	7.46	0.581	11	873	871
	7.47				
Rog 43	6.88	0.588	12	940	873
	6.87				
Rog 74	7.80	0.598	11	863	858
	7.81				
Rog 75	7.21	0.544	11	853	882
	7.19				
Rog 244	8.00	0.616	4	865	855
	8.01	0.613	4		
Rog 248	7.78	0.585	2	868	n.d.
	7.75	0.614	1		

* Error estimated at 3%, based upon estimated errors of 1% for K and 2% for Ar.

** Rb–Sr data published by Versteeve (1975), except for Rog 244 which was analyzed in this study (1283 and 1272 ppm Rb, 14.2 and 14.1 ppm Sr, and 5.3459 and 5.3565 for $^{87}Sr/^{86}Sr$). The ages were calculated with reference to the corresponding whole-rocks. Versteeve's ages were recalculated with the constants used in this study.

have been calculated, but recent studies on biotites along the front of the Caledonian nappe system in S. W. Norway indicate that the mineral has remained closed to Rb–Sr and K–Ar under a temperature as high as about 400°C (Verschure et al. 1979, 1980). This implies that after a relatively fast cooling subsequent to the M3 phase of metamorphism down to the blocking temperature of hornblende (550–490°C), it took some 80 Ma before the regional temperature had decreased another 100–150°C to the blocking temperature of the biotite (not less than about 400°C, assuming that the blocking temperature during cooling is approximately the same as the temperature at which biotite opens to Rb–Sr and K–Ar under conditions of rising temperature).

11. Tentative geochronological column

A provisional geochronological column of the high-grade metamorphic Precambrian in S. W. Norway has been set up by Versteeve (1975). On the basis of the additional observations of this study, also taking into account new data on the petrology and the field relations obtained by the Utrecht teams, the following, still tentative revised time framework is proposed for some of the major geological events:

Pre-Sveconorwegian

1. Deposition of a supracrustal sequence (sediments, volcanics) and intrusion of granites. Old radiogenic lead retained in some zircons may record traces of this early history. An event of metamorphism and/or magmatism about 1500 Ma ago (M0) may be recorded by a few zircon U–Pb and whole-rock Rb–Sr systems.

Sveconorwegian

2. *About 1200 Ma ago:* intrusion of the Botnavatn and Gloppurdi igneous complexes (mainly clinopyroxene syenites to granites), as registered by whole-rock Rb–Sr systems. Isotopic age data elsewhere in southern Norway indicate that the M1 phase of upper amphibolite facies metamorphism also probably took place at about this time, but no solid isotopic evidence has been found in the area under discussion.
3. *About 1050 Ma ago:* intrusion of the older phase of the Bjerkreim–Sokndal lopolith (the anorthositic to (leuconoritic) phase). The intrusion induced the M2 phase of high-temperature/intermediate-pressure granulite facies metamorphism over the greater part of the area. This event is recorded by the zircon U–Pb systems in the environmental high-grade basement.
4. *About 950 Ma ago:* intrusion of the younger phase of the Bjerkreim–Sokndal lopolith (the (quartz-)monzonitic phase), as registered by constituent zircon U–Pb and whole-rock Rb–Sr systems. Regional M3 phase of low granulite/upper amphibolite facies metamorphism, recorded by the whole-rock Rb–Sr systems of some suites of samples from the high-grade metamorphic basement. Following M3, the falling regional temperature passed the blocking temperature of hornblende to K–Ar, 550–490°C.
5. *About 870 Ma ago:* the falling regional temperature passed the blocking temperature of biotite to Rb–Sr and K–Ar, at least about 400°C.

Palaeozoic

6. *About 450—300 Ma ago:* M4 phase of incipient metamorphism in the pumpellyite-prehnite facies, in relation to the nearby belt of Caledonian orogenesis. Episodic loss of some radiogenic lead from the zircons took place due to this metamorphism and/or the post-orogenic uplift (dilatance), but the regional temperature remained below the temperature at which biotite opens to Rb–Sr and K–Ar.

The Sveconorwegian metamorphism in southwestern Scandinavia has nowhere reached such a high grade as in the Sirdal–Ørsdal area. This may be attributed to the conditions of the high-temperature/intermediate-pressure granulite facies, M2, which were induced over a great areal extent by the intrusion of the anorthositic to (leuco)noritic phase of the lopolith. Because of this high-grade metamorphism, very little has been preserved of any pre-Sveconorwegian isotopic age record.

Acknowledgements. – The authors are much indebted to Dr. C. Maijer, Prof. Dr. A. C. Tobi and Ir. G. A. E. M. Hermans, all from the Dept. of Petrology of Utrecht State University, and to Dr. R. P. Kuijper from the Z. W. O. Laboratorium voor Isotopen-Geologie, Amsterdam, for many helpful suggestions and stimulating discussions during the progress of the work. This study forms part of the research programme of the 'Stichting voor Isotopen-Geologisch Onderzoek', supported by the Netherlands Organization for the Advancement of Pure Research (Z. W. O.).

REFERENCES

Andriessen, P. A. M. 1978: Isotopic age relations within the polymetamorphic complex of the Island of Naxos (Cyclades, Greece). Verh. nr. 3 ZWO Laboratorium voor Isotopen-Geologie, Amsterdam, 72 pp.

Arden, J. W. & Gale, N. H. 1974: New electrochemical technique for the separation of lead at trace levels from natural silicates. *Anal. Chem. 46,* 2–9.

Barnes, I. L., Garner, E. L., Gramlich, J. W., Moore, L. J., Murphy, T. J., Machlan, L. A., Shields, W. R., Tatsumoto, M. & Knight, R. 1973: Determination of lead, uranium, thorium and thallium in silicate glass standard materials by isotope dilution mass-spectrometry. *Anal. Chem. 45,* 880–885.

Berg, Ø. 1977: En geokronologisk analyse av prekambrisk basement i distriktet Røldal–Haukelisæter–Valldalen ved Rb–Sr whole-rock metoden. Cand. real hovedoppgave (thesis), Univ. i Oslo.

Boelrijk, N. A. I. M., Kuijper, R. P. & Wielens, J. B. W. 1979a: Expressions for the calculation of error ellipses. Verh. nr. 4 ZWO Laboratorium voor Isotopen-Geologie, Amsterdam, 82–87.

Boelrijk, N. A. I. M., Kuijper, R. P. & Wielens, J. B. W. 1979b: Correlated errors and error ellipses in uranium-lead concordia diagrams. VIth European Colloquium on Geochronology, Cosmochronology and Isotope Geology, Lillehammer (Norway), September 3–6, 1979, Volume of Abstracts.

Corfu, F. 1978: Comparison of U–Pb systems in zircons, monazites and sphenes. A contribution to the geochronology of the Precambrian basement of central south Norway. IVth Int. Conf. on Geochronolgy, Cosmochronology and Isotope Geology, Snowmass-at-Aspen August 20–28, 1978, U. S. Geol. Surv. Open file report 78–701, 81–83.

Corfu, F. 1979: Response of U–Pb and Rb–Sr systems to Precambrian and Palaeozoic events in central South Norway. VIth European Colloquium on Geochronology, Cosmochronology and Isotope Geology, Lillehammer (Norway), September 3–6, 1979, Volume of Abstracts.

Dahlberg, E. H. 1969: Feldspars of charnockitic and related rocks. Rogaland, South-Western Norway, Ph. D. thesis Utrecht State University.

Daly, J. S., Park, R. G. & Cuff, R. A. 1979: Rb–Sr ages of intrusive plutonic rocks from the Stora Le–Marstrand belt in Orust, SW Sweden, Precambrian Res. 9, 189–198.

Dekker, A. G. C. 1978: Amphiboles and their host rocks in the high-grade metamorphic Precambrian of Rogaland/Vest-Agder, SW Norway. Geol. Ultraiectina 17, 277 pp. (Ph. D. thesis Utrecht State University).

Duchesne, J. C. & Demaiffe, D. 1978: Trace elements and anorthosite genesis. *Earth Planet. Sci. Lett. 38,* 479–482.

Goldich, S. S. & Mudrey, M. G. Jr. 1972: Dilatancy model for discordant U–Pb zircon ages. In: Contributions to recent geochemistry and analytical Chemistry (A. P. Vinogradov volume), A. I. Tugarinov (ed). Moscow, Nauka Publ. Office, 415–418.

Hart, S. R., Davis, G. L., Steiger, R. H. & Tilton, G. R. 1968: A comparison of the isotopic mineral age variations and petrological changes induced by contact metamorphism. In: Hamilton, E. I. and Farquhar, R. M. (eds) 1968: Radiometric dating for geologists. New York, Interscience Publ., 73–110.

Hermans, G. A. E. M., Tobi, A. C., Poorter, R. P. E. & Maijer, C. 1975: The high-grade metamorphic Precambrian of the Sirdal–Ørsdal area, Rogaland/Vest-Agder, SW Norway. *Norges geol. Unders. 318,* 51–74.

IJlst, L. 1973a: New diluents in heavy liquid mineral separation and an improved method for the recovery of the liquids from the washings. *Amer. Mineral. 58,* 1084–1087.

IJlst, L. 1973b: A laboratory overflow-centrifuge for heavy liquid mineral separation. *Amer. Mineral. 58,* 1088–1093.

Jäger, E., Niggli, E. & Wenk, E. 1967: Rb–Sr Altersbestimmungen an Glimmern der Zentralalpen. Beitr. Geol. Karte Schweiz, Nf Liefg. 134, Kümmerly and Frey, Bern.

Kratz, K. O., Gerling, E. K. & Lobach-Zhuchenko, S. B. 1968: The isotope geology of the Precambrian of the Baltic Shield. *Can. J. Earth Sci. 5,* 657–660.

Krogh, T. E. 1973: A low-contamination method for hydrothermal decomposition of zircon and extraction of U and Pb for isotopic age determinations. *Geochim. Cosmochim. Acta, 37,* 485–494.

Kuijper, R. P. 1979: U–Pb systematics and the petrogenetic evolution of infracrustal rocks in the Paleozoic basement of western Galicia (NW Spain). Verh. nr. 5 ZWO Laboratorium voor Isotopen-Geologie, Amsterdam, 101 pp.

Magnusson, N. H. 1965: The Precambrian history of Sweden. Quart. J. Geol. Soc. London 121, 1–30.

Maijer, C., Jansen, J. B. H., Hebeda, E. H., Verschure, R. H. & Andriessen, P. A. M. 1980: Osumilite, a 970 Ma old high-temperature index mineral of the granulite facies metamorphism in Rogaland, SW Norway. (In preparation).

McIntyre, G. A., Brooks, C., Compston, W. & Turek, A. 1966: The statistical assessment of Rb–Sr isochrons. *J. Geoph. Res. 71,* 5459–5468.

Michot, J. 1961: Le massif complex anorthosito-leuconoritique de Haaland–Helleren et le palingenèse basique. Mém. Acad. Roy. Belgique. Cl. Sci. 15, 95 p.

Michot, J. & Michot, P. 1969: The problem of anorthosites. The South-Rogaland igneous complex, southwestern Norway. In: Origin of anorthosite and related rocks, Y. W. Isachsen, ed., New York State Mus. Sci. Serv. Mem. 18, 399–410.

Michot, J. & Pasteels, P. 1968: Étude géochronologique du domaine métamorphique du sud-ouest de la Norvège. *Ann. Soc. Géol. Belg., 91,* 93–110.

Neumann, H. 1960: Apparent ages of Norwegian minerals and rocks. *Norsk geol. Tidsskr. 40,* 173–191.

Pasteels, P., Demaiffe, D. & Michot, J. 1979: U–Pb and Rb–Sr geochronology of the eastern part of the South Rogaland igneous complex. southern Norway. *Lithos 12,* 199–208.

Pasteels, P. & Michot, J. 1975: Geochronologic investigation of the metamorphic terrain of southwestern Norway. *Norsk geol. Tidsskr. 55,* 111–134.

Pasteels, P., Michot, J. & Lavreau, J. 1970: Le complexe éruptif du Rogaland méridional (Norvège). Signification pétrogénétique de la farsundite et de la mangérite quartzique des unités orientales; arguments géochronologiques et isotopiques. *Ann. Soc. Géol. de Belgique, 39,* 453–476.

Pedersen, S., Berthelsen, A., Falkum, T., Graversen, O., Hageskov, B., Maaløe, S., Petersen, J. S., Skjernaa, L. & Wilson, J. R. 1978: Rb/Sr dating of the plutonic and tectonic evolution of the Sveconorwegian province, southern Norway. U.S. Geol. Surv. Open file report 78–701, 329–331.

Reymer, A. P. S., Boelrijk, N. A. I. M., Hebeda, E. H., Priem, H. N. A., Verdurmen, E. A. Th. & Verschure, R. H. 1980: Northward extension of the Sveconorwegian 'front' along the coast of Norway: evidence from Rb–Sr whole-rock investigation in the Seve Nappe of the central Scandinavian Caledonides. *Norges geol. Tidsskr. 60* (in press),

Rietmeijer, F. J. M. 1979: Pyroxenes from iron-rich igneous rocks in Rogaland, SW Norway. Geol. Ultraiectina 21, 341 pp. Ph. D. thesis Utrecht State University.

Schaerer, U. 1978: Rock deformation and zircon-sphene U–Ph dating. U.S. Geol. Surv. Open file report 78–701, 380–382.

Shields, W. R., ed., 1966: Technical note no 227 U. S. National Bureau of Standards.

Sigmond, E. M. O. 1978: Beskrivelse til det berggrunnsgeologiske kartbladet Sauda 1 : 250.000 (Med fargetrykt kart). *Norges geol. Unders. 341,* 1–94.

Skiöld, T. 1976: The interpretation of the Rb–Sr and K–Ar ages of late Precambrian rocks in south-western Sweden. Geol. Fören. Stockh. Förh. 98, 3–29.

Sommerauer, J. 1976: Die chemisch-physikalische Stabilität natürlicher Zirkone und ihr U–(Th)–Pb System. Dissertation Nr. 5755 Eidg. Techn. Hochschule, Zürich, 151 pp.

Stacey, J. S. & Kramers, J. D. 1975: Approximation of terrestrial lead isotope evolution by a two-stage model. *Earth Planet. Sci. Lett. 26,* 207–221.

Swainbank, I. 1965: Zircon geochronology of the Norwegian basement. Annual Progr. Rep. nr. 10 Contract AT(30–1)–1669, Lamont Geological Observatory, App. C.

Tobi, A. C. 1965: Fieldwork in the charnockitic Precambrian of Rogaland (SW Norway).

Geol. Mijnb. 44, 207–217.
Verdurmen, E. A. Th. 1977: Accuracy of X-ray fluorescence spectrometric determination of Rb and Sr concentrations in rock samples. X-Ray Spectr. 6, 117–122.
Verschure, R. H., Andriessen, P. A. M., Boelrijk, N. A. I. M., Hebeda, E. H., Maijer, C., Priem, H. N. A. & Verdurmen, E. A. Th. 1979: Coexisting primary biotite of Sveconorwegian age and secondary biotite of Caledonian age in Sveconorwegian basement rocks close to the Caledonian front in S.V. Norway. VIth European Colloquium on Geochronology, Cosmochronology and Isotope Geology, Lillehammer (Norway), September 3–6, 1979, Volume of Abstracts.
Verschure, R. H., Andriessen, P. A. M., Boelrijk, N. A. I. M., Hebeda, E. H., Maijer, C., Priem, H. N. A. & Verdurmen, E. A. Th. 1980: On the thermal stability of Rb–Sr and K–Ar biotite systems: evidence from coexisting Sveconorwegian (ca 870 Ma) and Caledonian (ca 400 Ma) biotites in S.W. Norway. Contr. Petrol. Mineral. (in press).
Verschure, R. H. & IJlst, L. 1966a: The 'Intracentrifuge', a device for continuous separation of heavy minerals. *Min. Mag. 35,* 1165–1167.
Verschure, R. H. & IJlst, L. 1966b: Apparatus for continuous dielectric-medium separation of mineral grains. *Nature 211,* 619–620.
Verschure, R. H. & IJlst, L. 1969: An improved assymetrically vibrating unit for the Frantz magnetic separator. Reports on Investigations in the year September 1968 to September 1969, ZWO Laboratorium voor Isotopen-Geologie, Amsterdam, 90.
Versteeve, A. J. 1975: Isotope geochronology in the high-grade metamorphic Precambrian of Southwestern Norway. *Norges geol. Unders. 318,* 1–50.
Welin, E. 1974: Summary of a lecture on the Precambrian geochronology of Sweden. Geologi, 26 vsk, N 3, 34.
Welin, E. & Gorbatschev, R. 1978a: Rb–Sr age of the Lane granites in south-western Sweden. Geol. Fören. Stockh. Förh. 100, 101–102.
Welin, E. & Gorbatschev, R. 1978b: The Rb–Sr age of the Varberg charnockite, Sweden. Geol. Fören. Stockh. Förh. 100, 225–227.
Welin, E. & Gorbatschev, R. -978c: Rb–Sr isotope relations of a tonalite intrusion on Tjörn Island, south-western Sweden. Geol. Fören. Stockh. Förh. 100, 228–230.
Wielens, J. B. W. 1979: Morphology and U–Pb ages from the high-grade metamorphic Precambrian in the Sirdal–Ørsdal area, SW Norway. Verh. nr. 4 ZWO Laboratorium voor Isotopen-Geologie, Amsterdam, 1–79.
Wielens,, J. B. W., van Belle, K., Boelrijk, N. A. I. M. & Kuijper, R. P. 1979: Chemical procedure for U–Pb dating. Verh. nr. 4 ZWO Laboratorium voor Isotopen-Geologie, Amsterdam, 80–81.
York, D. 1966: Least-squares fitting of a straight line. *Can. J. Phys. 44,* 1079–1086.
York, D. 1967: The best isochron. *Earth Planet. Sci. Lett. 2,* 479–482.
York, D. 1969: Least squares fitting of a straight line with correlated errors. *Earth Planet Sci. Lett. 5,* 320–324.